Thiolene-based microfluidic flow cells for surface plasmon resonance imaging

Gareth Sheppard, Takao Oseki, Akira Baba, Derek Patton, Futao Kaneko et al.

Citation: Biomicrofluidics **5**, 026501 (2011); doi: 10.1063/1.3596395
View online: http://dx.doi.org/10.1063/1.3596395
View Table of Contents: http://bmf.aip.org/resource/1/BIOMGB/v5/i2
Published by the American Institute of Physics.

Thiolene-based microfluidic flow cells for surface plasmon resonance imaging

Gareth Sheppard,[1] Takao Oseki,[2] Akira Baba,[3] Derek Patton,[4] Futao Kaneko,[2] Leidong Mao,[5,a)] and Jason Locklin[1,a)]
[1]*Department of Chemistry, Faculty of Engineering, Nanoscale Science and Engineering Center, University of Georgia, Athens, Georgia 30602, USA*
[2]*Graduate School of Science and Technology, Niigata University, 8050, Igarashi 2-Nocho, Nishi-ku, Niigata 950-2181, Japan*
[3]*Center for Transdisciplinary Research, Niigata University, 8050, Igarashi 2-Nocho, Nishi-ku, Niigata 950-2181, Japan*
[4]*School of Polymers and High Performance Materials, University of Southern Mississippi, Hattiesburg, Mississippi 39406, USA*
[5]*Faculty of Engineering, Nanoscale Science and Engineering Center, University of Georgia, Athens, Georgia 30602, USA*

(Received 1 March 2011; accepted 1 May 2011; published online 7 June 2011)

Thiolene-based microfluidic devices have been coupled with surface plasmon resonance imaging (SPRI) to provide an integrated platform to study interfacial interactions in both aqueous and organic solutions. In this work, we develop a photolithographic method that interfaces commercially available thiolene resin to gold and glass substrates to generate microfluidic channels with excellent adhesion that leave the underlying sensor surface free from contamination and readily available for surface modification through self-assembly. These devices can sustain high flow rates and have excellent solvent compatibility even with several organic solvents. To demonstrate the versatility of these devices, we have conducted nanomolar detection of streptavidin-biotin interactions using *in situ* SPRI. © *2011 American Institute of Physics.* [doi:10.1063/1.3596395]

I. INTRODUCTION

Surface plasmon resonance imaging (SPRI) is a label-free detection technique that can provide real-time monitoring of spatially resolved refractive index changes that occur near a noble metal surface.[1–7] SPRI devices use a CCD camera to monitor the reflected light, which is sensitive to differences in refractive index (RI) and film thickness at the sensor's interface. This technique is extremely powerful in that real-time kinetic and thermodynamic analysis of surface and interfacial interactions can be monitored.[3–6,8–12] It is also amenable to parallel analysis of adsorption events in an array format.[13,14] Rapid analyses of biomolecular interactions using SPRI arrays have been investigated recently.[15–18] Coupling SPRI with microfluidics provides an integrated platform for *in situ* biomolecular studies while greatly reducing the consumption of sample reagents.[11,19–22] Poly(dimethylsiloxane) (PDMS) is a widely used material in the fabrication of microfluidic devices with aqueous systems due to its excellent optical properties, biocompatibility, air permeability, and low cost.[14,23–27] However, PDMS devices perform poorly with the introduction of organic solvents into the channels, resulting in solvent leakage or swelling.[23,28,29] Swelling of PDMS can lead to significant changes in the cross-sectional area of microchannels, which can alter the flow rates and flow dynamics, leaching of uncured monomers from the sidewalls into the channel or sensor surface, cross-contamination of adjacent microchannels, leakage of solvents, and, ultimately, device failure. The incompatibility between PDMS and organic solvents also limits the

a)Authors to whom correspondence should be addressed. Electronic mail: mao@uga.edu. Tel.: 1-706-542-1871. FAX: 1-706-542-3804 and Electronic mail: jlocklin@uga.edu. Tel.: 1-706-542-2359. FAX: 1-706-542-3804.

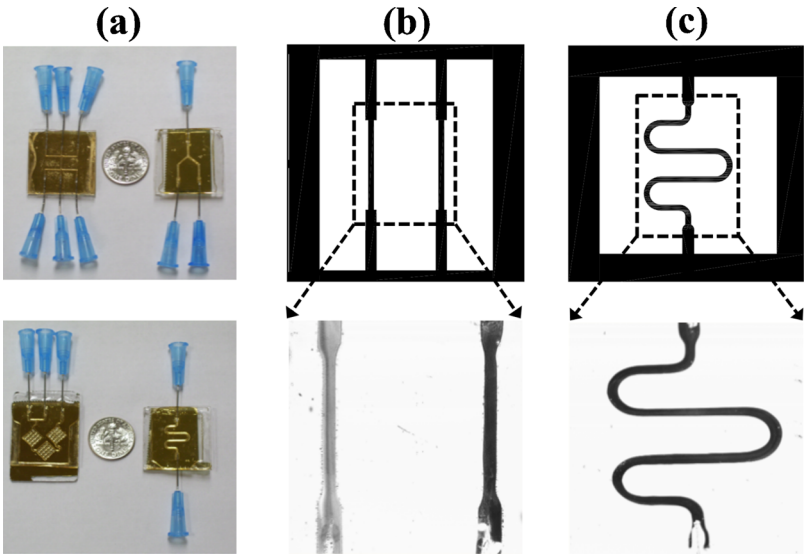

FIG. 1. (a) The fabricated microfluidic devices with dime-sized imaging windows. (b) Mask design (top) and SPR image (bottom) of straight channels. The SPR image compares channels filled with water (left) to isopropanol (right). The difference in pixel intensity is due to the refractive index mismatch of two solutions. (c) Mask design (top) and SPR image (bottom) of serpentine channel. SPR image was taken using PBS. The width of channels in (b) and (c) is 600 μm; the thickness is 1000 μm.

variety of chemical processes that can be performed in microfluidic devices, particularly when interfaced to a gold substrate, where the adhesion is very weak. This is a limiting factor when developing microchannels for SPRI applications, even for aqueous systems, since surface functionalization of the channels typically starts with an organic-phase alkane thiol modification step.

Due to solvent incompatibility and adhesion difficulties between PDMS and Au substrates, an alternative material is necessary to develop organic-phase-based microfluidic devices. Thiolene-based optical adhesives are excellent candidates for these applications as they have provided excellent versatility and solvent compatibility in both water and a wide variety of nonhalogenated organic solvents.[28,30] Rapid prototyping with commercially available thiolene resins allows simple fabrication of microfluidic devices with feature sizes as small as 70 μm.[28,30–32] However, current fabrication techniques of thiolene-based microfluidic devices present challenges for their integration with SPRI systems. Thiolene resins bind strongly to gold surfaces through free thiols, making reproducible functionalization of gold sensor surfaces arduous. In this study, we have developed an alternative strategy of fabricating thiolene-based microfluidic devices and successfully integrated them with a SPRI system without contaminating the sensor surface. As a proof of concept, we demonstrated the reproducible functionality of the sensor surface using a common binding assay of biotinylated monolayers and streptavidin (SA). The devices were also able to sustain high flow rates with very limited swelling effects and no solvent leakage in several organic solvents. Samples of finished microfluidic devices are shown in Fig. 1(a). Figures 1(b) and 1(c) depict representative mask designs of microfluidic channels and the corresponding SPR images of solvents within the channels.

II. DEVICE FABRICATION

Standard photolithographic techniques require ultraclean environments and typically involve negative master molds. The method used in this work utilizes standard office equipment to produce a variety of microfluidic designs that do not require a master mold for replication nor clean room facilities. Figures 2(a)–2(e) show the materials and fabrication process of thiolene-based microfluidic devices.

Masks of microfluidic devices were drawn to scale using AUTOCAD (Autodesk Inc., San

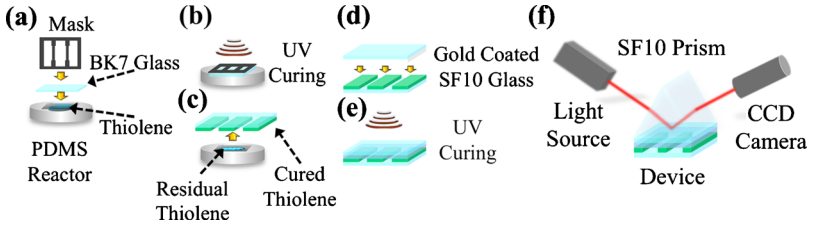

FIG. 2. [(a)–(e)] Thiolene microfluidic device fabrication scheme. Transparency printed mask was taped to a BK7 glass slide before being placed onto thiolene filled PDMS reactor. Exposure to UV light photopolymerized the thiolene resin and formed the microfluidic channels. A gold-coated SF10 slide was used to cap the channels. (f) The experimental setup followed the Kretschmann configuration where the SF10 prism and device were coupled using refractive index matching fluid. Images are collected using a CCD camera.

Rafael, CA) and printed on laser transparency films with a commercial laser printer (HP LaserJet 1022, 1200 DPI). The transparency mask was taped to a glass slide for selective photopolymerization of thiolene resin (NOA 81 optical adhesive, Norland Product Inc., Cranbury, NJ), which occur under ultraviolet (UV) light exposure. Polymerization occurs where the UV radiation passes through the mask, the channels formed from masked areas where the radiation is blocked. The microfluidic channel thickness depends on the UV light penetration into liquid thiolene. It has been observed previously that the maximum penetration depth is 63.5 cm.[33] A PDMS "reactor" was used to cure the thiolene because of very poor adhesion between thiolene and PDMS. The reactor was formed from a mixture of silicone elastomer base and curing agent (Sylgard 184 Kit, Dow Corning, Hemlock, MI) in a 10:1 mass ratio. Degassed PDMS is poured over a glass slide or silicon wafer, 1.0 mm and 0.5 mm thick, cut to the desired reactor size, and cured at 70 °C for 2 h. Once cured, the spacer slide is removed, leaving a uniform reactor. The PDMS reactor can be filled with thiolene resin, as shown in Fig. 2(a).

During device fabrication, the mask was attached to a BK7 glass (RI of 1.515 at $\lambda = 632.8$ nm) slide and lowered into contact with the thiolene resin filled PDMS reactor, as shown in Fig. 2(a). An UV light source was used to photopolymerize the thiolene resin with 200 $\mu W/cm^2$ power for 4.5 min [Fig. 2(b)]. After exposure, the thiolene resin was cured onto the glass slide and separated from the PDMS reactor to form microfluidic channels. The channels were first rinsed with ethanol to remove any uncured material and then rinsed with acetone, followed by ethanol again before drying with a moderate flow rate of nitrogen gas. A secondary curing of the thiolene resins was performed with 1 min UV exposure at 200 $\mu W/cm^2$ power. A thin film of thiolene was then carefully sprayed over cured thiolene patterns with a thin layer chromatography sprayer, providing a curable surface to bind to a gold-coated SF10 glass slide (RI of 1.723, $\lambda = 632.8$ nm). This is shown in Fig. 2(d). The gold layer on the SF10 glass slides was deposited by thermal evaporation using 1 nm thick chromium and 47 nm thick gold. The gold-coated SF10 glass slide was pressure sealed against the thiolene microfluidic channels on the BK7 glass slide and UV cured to form the final device [Fig. 2(e)]. Needles are then inserted and sealed at channel openings by applying thiolene resin and exposing to UV at 3 mW/cm^2. Exposing at a higher power setting ensures complete polymerization and reduces the amount of residual monomer in the completed device. The final device is heat cured at 50 °C for 12 h. Overall, the device design and fabrication is low cost and can be completed within several hours.

III. SURFACE PLASMON RESONANCE IMAGING

A SPRI system (SPRImager II, GWC Technologies, Madison, MI), which is consist of a white light source with a 800 nm narrow band pass filter, polarizer, and a CCD camera, was used for the *in situ* experiments. The finished thiolene-based microfluidic device was attached to the rotating stage of the SPRI system with a custom-made holder in the Kretschmann configuration.[5,7,9,34] The light source of the SPRI system excited surface plasmon resonance at an angle intrinsic to the metal and substrate layers, as shown in Fig. 2(f). A peristaltic pump was used to control the rate

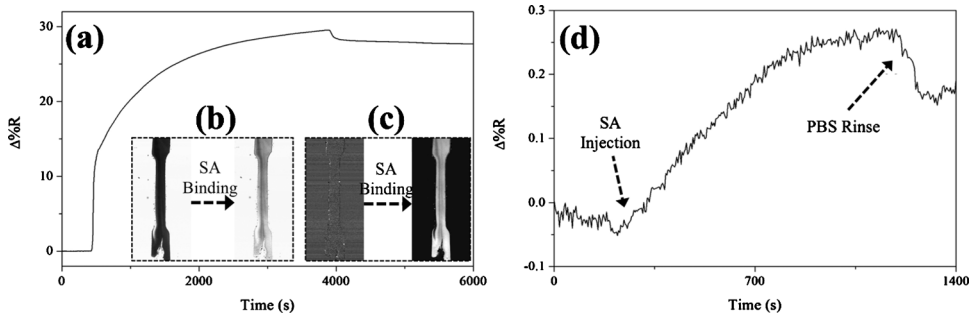

FIG. 3. (a) Streptavidin (75 μM) binding to biotin functionalized monolayers on glass surface. SPR images (b) and difference images (c) taken before and after streptavidin flow in the recycle mode. Unbound streptavidin was removed by PBS rinse at 65 min. (d) A low concentration of streptavidin (150 nM) injected over biotin functionalized monolayers on gold surface. Unbound streptavidin was removed by PBS rinse at 20 min.

of fluid flow through the microfluidic device. The system was set up to recycle fluid from the outlets back into the inlets, reducing the required volume to that of the microfluidic channel and connected tubing, totaling to 1.0 ml for each solution. Upon changing solutions, the system was taken out of the recycle mode. The SPR signal intensity changes when the new solution passes across the sensor; from the flow rate and the remaining tubing volume the time to place the system back into recycle mode can be calculated preventing cross-contamination of the solutions.

The binding of SA to a biotinylated monolayer was used to determine the working parameters and detection limits of the microfluidic device with the SPRI system. Streptavidin has a tetrameric structure with high affinity to biotin.[34] A thiolene microfluidic device with 600 μm $\times$ 1000 μm (aspect ratio: 1.67) was fabricated for the SA sensing. In order to coat the gold surface with biotin, a self-assembled monolayer was first deposited onto the gold by flowing 10 mM 11-mercaptoundecanoic acid (11-MUA) solution in ethanol through the microfluidic channels for 1.5 h. The channels were rinsed with ethanol, followed by isopropanol and de-ionized water for 30 min. Phosphate buffer solution (PBS) was flowed through the channels to ensure that any solvent mixing and the resulting refractive index change were minimized. A mixture of 0.2*M* 1-ethyl-3-(3-dimethylaminopropyl) carbodiimide hydrochloride and 0.05*M* *N*-hydroxysuccinimide was used to activate the carboxyl groups for reaction with amine terminated biotin. Finally, a solution containing 1 mg/ml amine-PEG3-biotin in PBS was flowed through the device at 3 μl/s for 1.5 h to coat the gold surface with biotin. Finally, streptavidin in PBS was flowed through the device at 3 μl/s and the binding events were monitored in real-time by the SPRI system.

During the final PBS rinse, a thiolene microfluidic device attached on the rotating stage was adjusted to find the SPR minimum and then shifted 1°–2° to the left for the optimal imaging angle. Reference images are taken and regions of interest were selected, covering the channel for kinetics tracking. Subsequent SPR images are compared to the reference images from which the change in percent reflectivity (Δ%R) due to a binding event is monitored by difference image analysis.

IV. RESULTS AND DISCUSSION

A thiolene microfluidic device consisting of 600 μm wide channels was used to evaluate the binding kinetics of 75 μM streptavidin with a biotinylated monolayer, as depicted in Fig. 3(a). The initial 500 s of the plot was PBS flow prior to streptavidin injection. The reflectivity difference before and after streptavidin injection clearly demonstrated that the gold surface was successfully functionalized with biotin, and the streptavidin was able to bind to biotin on the gold surface. Figure 3(b) compared a SPR image taken before streptavidin injection to an image taken after streptavidin flow for 100 min in recycle mode. Streptavidin-biotin binding shifted the SPR minimum to a larger angle, resulting in a clear reflectivity change as demonstrated by the pixel

TABLE I. A swelling ratio ($S=W/W_0$) describes the amount of swelling or delamination due to solvent-thiolene interaction, a value of 1 denotes no change. S^{α} denotes microfluidic channel swelling after 2 h. S^{β}, solvent swelling on 2 mm squares of thiolene after 24 h. Thiolene swelling ratios are compared to PDMS's swelling ratio previously reported, S^{γ}, for 24 h. For channel swelling, S^{α}, the initial width is larger than the final width, resulting in values less than unity.

	S^{α}	S^{β}	S^{γ}
H_2O	1.01 ± 0.02	1.01 ± 0.00	1.00
Acetonitrile	⋯	1.11 ± 0.01	1.01
Ethyl Ether	⋯	0.99 ± 0.01	1.38
Acetone	1.02 ± 0.03	1.12 ± 0.01	1.06
Ethanol	1.03 ± 0.03	1.00 ± 0.01	1.04
Ethyl acetate	1.04 ± 0.02	⋯	1.18
Hexane	1.03 ± 0.04	1.00 ± 0.01	1.35
Isopropanol	0.93 ± 0.04	1.00 ± 0.00	1.09[a]
Tetrahydrofuran	0.92 ± 0.01	1.16 ± 0.04	1.38
Dichloromethane	⋯	1.27 ± 0.03	1.22
Chloroform	⋯	1.34 ± 0.03	1.39
Toluene	⋯	1.02 ± 0.02	1.31

[a]Value for 1-propanol.

intensity level. Demonstrated in Fig. 3(c) are the difference images from which kinetic data are taken and provided ocular confirmation of the protein binding events allowing for high throughput protein sensing.

The detection limit of streptavidin-biotin binding was characterized with a 150 nM streptavidin solution, as shown in Fig. 3(d). Buffer solution is used to determine baseline reflectivity values prior to and after binding. After the initial SA binding, the peristaltic pump was stopped to allow for diffusion-limited binding to take place. The characteristic binding curve demonstrates the ability of thiolene-based microfluidics to detect 5.4 ng/mm^2 of protein with an approximate limit of detection at 10 nM (0.4 ng/mm^2) in this system.

Thiolene microfluidic devices are more versatile in solvent compatibility than PDMS. Solvent compatibility can be expressed in terms of a swelling ratio, $S=W/W_0$, where W_0 is the initial width and W is the width after solvent exposure.[29] Various solvents were passed through the thiolene microfluidic device for 2 h to monitor thiolene swelling or delamination, S^{α} in Table I. For channel swelling, values greater than 1 indicate delamination and values less than unity indicate swelling. SPR images of the channel were taken before and after exposure to solvent and the distance between the channel walls were measured using the number of pixels. A 24 h swelling study on 2 mm square thiolene pieces, S^{β}, was also performed to compare directly to PDMS swelling ratios, S^{γ} found in Ref. 25. In the 24 h study, thiolene squares were imaged with a microscope (Zeiss, AXIO Imager A2) using a 2.5× lens. For each solvent, three squares were measured and the edge-to-edge distance was computed. Initial distances were determined from images taken prior to solvent exposure. After 24 h, the squares were imaged while still in solution to reduce the chances of deswelling associated with solvent evaporation. A value greater than 1 from the 24 h experiment indicates the increase in size due to swelling effects. With little variation around unity for a majority of the solvents in Table I, the performance of the thiolene devices is excellent for most organic solvents. For halogenated solvents dichloromethane and chloroform, swelling causes the square to increase by 30% along any given Cartesian coordinate. Solvents such as tetrahydrofuran can be used for limited time frames as indicated by the difference in S^{α} and S^{β}. Another important contrast is that thiolene microfluidic devices are compatible with certain organic solvents that PDMS is not, such as hexane, toluene, and ethyl ether.

V. CONCLUSIONS

A simple, low-cost thiolene microfluidic device has been designed and fabricated to allow integration with SPRI systems with a wide range of solvents. Thiolene microfluidics is a robust tool for applications where PDMS devices fail, such as high pressure or applications that involve the use of organic solvents. These devices provide microfluidic channels with excellent adhesion and leave the underlying sensor surface free from contamination. Thiolene devices can sustain high flow rates and have excellent solvent compatibility even with several organic solvents. The advantage of using organic solvents with negligible swelling effects or channel leakage is that it further increases versatility and utility of these devices for sensor applications on the microliter scale.

[1] R. Pei, X. Yang, and E. Wang, Analyst (Cambridge, U.K.) **126**, 4 (2001).
[2] M. Harke, R. Teppner, O. Schulz, H. Motschmann, and H. Orendi, Rev. Sci. Instrum. **68**, 3130 (1997).
[3] S.-J. Kim, K. Vengatajalabathy Gobi, H. Iwasaka, H. Tanaka, and N. Miura, Biosens. Bioelectron. **23**, 701 (2007).
[4] Z. Wang, T. Wilkop, D. Xu, Y. Dong, G. Ma, and Q. Cheng, Anal. Bioanal. Chem. **389**, 819 (2007).
[5] N. Ly, K. Foley, and N. Tao, Anal. Chem. **79**, 2546 (2007).
[6] H. V. Hsieh, B. Stewart, P. Hauer, P. Haaland, and R. Campbell, Vaccine **16**, 997 (1998).
[7] Y. Iwasaki, T. Tobita, K. Kurihara, T. Horiuchi, K. Suzuki, and O. Niwa, Meas. Sci. Technol. **17**, 3184 (2006).
[8] R. B. M. Schasfoort, Expert Rev. Proteomics **1**, 123 (2004).
[9] K.-H. Lee, Y.-D. Su, S.-J. Chen, F.-G. Tseng, and G.-B. Lee, Biosens. Bioelectron. **23**, 466 (2007).
[10] R. Georgiadis, K. P. Peterlinz, and A. W. Peterson, J. Am. Chem. Soc. **122**, 3166 (2000).
[11] H. J. Lee, T. T. Goodrich, and R. M. Corn, Anal. Chem. **73**, 5525 (2001).
[12] H. J. Lee, A. W. Wark, and R. M. Corn, Langmuir **22**, 5241 (2006).
[13] K. A. Heyries, M. G. Loughran, D. Hoffmann, A. Homsy, L. J. Blum, and C. A. Marquette, Biosens. Bioelectron. **23**, 1812 (2008).
[14] M. Herrmann, E. Roy, T. Veres, and M. Tabrizian, Lab Chip **7**, 1546 (2007).
[15] J. M. Brockman, B. P. Nelson, and R. M. Corn, Annu. Rev. Phys. Chem. **51**, 41 (2000).
[16] J. Liu, M. A. Eddings, A. R. Miles, R. Bukasov, B. K. Gale, and J. S. Shumaker-Parry, Anal. Chem. **81**, 4296 (2009).
[17] C. F. Grant, V. Kanda, H. Yu, D. R. Bundle, and M. T. McDermott Langmuir **24**, 14125 (2008).
[18] M. Dhayal and D. M. Ratner, Langmuir **25**, 2181 (2009).
[19] G. J. Wegner, A. W. Wark, H. J. Lee, E. Codner, T. Saeki, S. Fang, and R. M. Corn, Anal. Chem. **76**, 5677 (2004).
[20] Y. Luo, F. Yu, and R. N. Zare, Lab Chip **8**, 694 (2008).
[21] E. A. Smith, W. D. Thomas, L. L. Kiessling, and R. M. Corn, J. Am. Chem. Soc. **125**, 6140 (2003).
[22] J. D. Taylor, M. J. Linman, T. Wilkop, and Q. Cheng, Anal. Chem. **81**, 1146 (2009).
[23] M. Natali, S. Begolo, T. Carofiglio, and G. Mistura, Lab Chip **8**, 492 (2008).
[24] G. M. Whitesides, Nature (London) **442**, 368 (2006).
[25] W.-C. Sung, C.-C. Chang, H. Makamba, and S.-H. Chen, Anal. Chem. **80**, 1529 (2008).
[26] J. C. McDonald and G. M. Whitesides, Acc. Chem. Res. **35**, 491 (2002).
[27] A. Tirella, M. Marano, F. Vozzi, and A. Ahluwalia, Toxicol. In Vitro **22**, 1957 (2008).
[28] Z. T. Cygan, J. T. Cabral, K. L. Beers, and E. J. Amis, Langmuir **21**, 3629 (2005).
[29] J. N. Lee, C. Park, and G. M. Whitesides, Anal. Chem. **75**, 6544 (2003).
[30] T. Wu, Y. Mei, J. T. Cabral, C. Xu, and K. L. Beers, J. Am. Chem. Soc. **126**, 9880 (2004).
[31] J. T. Cabral, S. D. Hudson, C. Harrison, and J. F. Douglas, Langmuir **20**, 10020 (2004).
[32] B. Vogel, J. T. Cabral, N. Eidelman, B. Narasimhan, and S. K. Mallapragada, J. Comb. Chem. **7**, 921 (2005).
[33] N. B. Cramer, J. P. Scott, and C. N. Bowman, Macromolecules **35**, 5361 (2002).
[34] O. Azzaroni, M. Mir, and W. Knoll, J. Phys. Chem. B **111**, 13499 (2007).